ELSEVIER

20 June 1997

Chemical Physics Letters 272 (1997) 18–24

CHEMICAL PHYSICS LETTERS

Charge-exchange collisions of C_{60}^{z+}: a probe of the ion charge distribution

Douglas B. Cameron, Joel H. Parks

Rowland Institute for Science, 100 Edwin H. Land Blvd., Cambridge, MA 02142-1297, USA

Received 25 February 1997

Abstract

We present Paul trap measurements of charge-exchange collisions of Li, Cs and C_{60} with C_{60}^{z+} ions ($z = 1$–3) at thermal energies. Surprisingly, the measured charge-exchange rates for each neutral species are not proportional to the ion charge z as would be expected for Langevin collisions involving a uniformly charged ion. The relative rates can be reproduced by a model based on a symmetric distribution of point charges that are free to move on the ion surface during the neutral trajectory. Such behavior can be attributed to static and possibly dynamic Jahn–Teller effects in C_{60}^{z+} ions. © 1997 Elsevier Science B.V.

1. Introduction

Multiply-charged C_{60}^{z+} ions provide a unique opportunity to observe charge-exchange interactions which exhibit a strong dependence on the distribution and mobility of charge on the molecular microsurface. Since the diameter of C_{60} (≈ 7 Å) is comparable to the range of the ion–neutral interaction during collisions, it might be expected that the collision dynamics depend on characteristics of the ion charge distribution. Studies of low energy charge-exchange between C_{60}^{+} and alkali atoms [1] and of C_{60}^{2+} with small molecules [2] have suggested models of a charge distribution that included charge motion on the ion microsurface during the interaction trajectory. A symmetric distribution of $+z$ point charges on the C_{60} surface was proposed by Bohme and co-workers [3] to describe the charge-exchange process from C_{60}^{z+} ions and was applied to experimental results of fission (dissociation) reactions with $3 \leqslant z \leqslant 7$ by Märk and co-workers [4].

This Letter presents experimental results which relate the long range ion–neutral interaction to the ion charge distribution. Our results are not expected to depend on the details of the curve-crossing dynamics where charge-exchange occurs. These crossings are estimated to occur at ion–neutral separations shorter than the Langevin critical capture distance arising in ion–induced dipole collisions. This is in contrast to the measurements of C_2^{+} fission [4] which require a model of the C_{60}^{z+} ion distribution at the point of charge separation to estimate the fission dynamics. However, both fission and the collision interactions of C_{60}^{z+} can be described with a distribution of equidistant point charges on the ion surface. In addition, the collision rates obtained from our experiments imply that the charge distribution is free to undergo rigid rotation about the C_{60} microsurface during the collision trajectory. The experimental implications of a nonuniform charge distribution and its apparent rapid rotation during the collision are discussed in the context of Jahn–Teller effects, previ-

0009-2614/97/$17.00 © 1997 Elsevier Science B.V. All rights reserved.
PII S0009-2614(97)00498-3

ously studied for anions, cations and neutral triplet states of C_{60}.

2. Experiment

The experimental arrangement used for these measurements has been described elsewhere [1,5]. C_{60}^{z+} ions and C_{60-2m}^{z+} fragments were loaded into a radio frequency Paul trap by electron ionization of an effusive beam of C_{60} entering through an aperture in the ring electrode. Multiply charged ions ($\leqslant 10^3$ ions) were produced by an electron beam current density of ≈ 2 mA/cm^2 at ≈ 100 eV energy for exposure times of 0.5–1 s. The trap was maintained at 300 K and ions were stored within a background He gas at pressures of $\approx 10^{-4}$ Torr, adequate to thermalize the translational and vibrational degrees of freedom [1]. The ions were then exposed to a thermal beam of alkali atoms or C_{60} molecules that traverses the trap through two apertures in the ring electrode for an exposure interval set by a solenoid driven shutter.

Charge-exchange collisions between C_{60}^{z+} ions and alkali atoms resulted in a decay of the number of trapped ions. Previous experiments [1] demonstrated that this was the only significant process responsible for ion decay. The trapped ion lifetime was several minutes in the absence of neutral flux and contributed negligible loss to these measurements. After exposing the trapped ions to the neutral beam for a specific time interval, the number of remaining ions was determined by resonantly ejecting all trapped ions into an electron multiplier. Simultaneous measurements on ions having different charge states z could be made by trapping a range of m/z ions. This allowed an accurate determination of the decay rates of C_{60}^{z+} relative to C_{60}^{+}. These relative rates eliminate the dependence on the neutral flux which, although required for absolute rates, was found to be difficult to calibrate accurately [1]. Fig. 1 displays the mass spectrum of trapped ions before exposure to neutral flux. The trapped ion spectrum in Fig. (1) spans a trap parameter range of $0.21 \leqslant q_z \leqslant 0.84$ and the number of ions for each species is proportional to the integrated peak signal. By performing these measurements as a function of exposure interval, the relative charge-exchange rate of each ion species was determined.

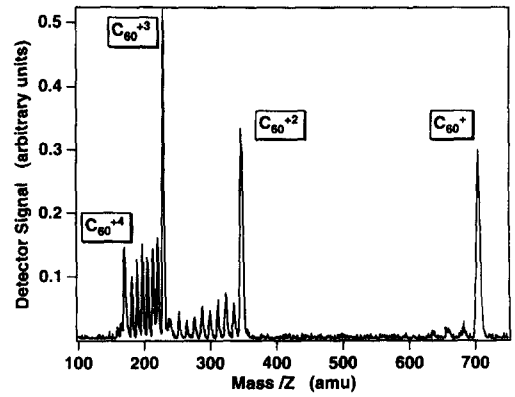

Fig. 1. The mass spectrum of trapped C_{60}^{z+} and associated fragments are shown. Ions are loaded into the trap by e-beam ionization of neutral C_{60} and the spectrum is detected by resonant ejection of the ions into an electron multiplier.

The charge-exchange channels observed in these experiments resulted from reactions

$$C_{60-2m}^{z+} + M \rightarrow C_{60-2m}^{(z-1)+} + M^{+} \quad M = \mathrm{Li, Cs, C_{60}} \tag{1}$$

for $z = 1$–4, $m = 0$–5. Resonant ion ejection from the Paul trap permitted either individual masses or mass distributions to be isolated for study. When C_{60}^{+} or C_{60}^{2+} was mass isolated in the trap prior to exposure, the decay of either ion was observed to be a single exponential extending over 2–3 orders of magnitude. However, exposure of the complete multiply-charged mass spectrum shown in Fig. 1 results in more complex behavior since it includes the cascade of ions to lower charge states.

Charge-exchange rates were extracted from the analysis of multiply-charged mass spectra by comparing the measured time dependent population of each species with the solution of a coupled set of differential equations involving collision rate parameters. The decay rate of each species was then independently determined as fit parameters to these solutions. As an example, the decay of C_{60}^{z+} ions ($z =$ 1–3) during Li flux exposure is shown in Fig. 2. Each data point is an average of ≈ 5 measurements and exhibits scatter arising from statistical fluctuations. The cascade of $+2$ to $+1$ ions is clearly evident in the initial increase of the $+1$ species. The experimental rates derived from exponential fits of the decay curves shown in Fig. 2 are $k_1 = 1.88$ s^{-1},

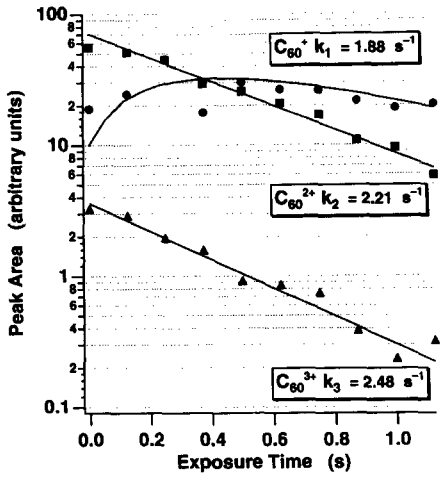

Fig. 2. The decay curves for charge-exchange of C_{60}^{z+} with Li are shown for $z=1$ by filled circles, $z=2$ by filled squares and $z=3$ by filled triangles. The solid curves are determined by parameter fits of the decay rates k_1, k_2 and k_3 shown next to curve. The data points were obtained by integrating the mass spectrum peaks of C_{60}^{z+} for each charge state z at each Li exposure time.

$k_2 = 2.21\ s^{-1}$, $k_3 = 2.48\ s^{-1}$ for $z = +1, +2, +3$ respectively with an uncertainty of $\pm 15\%$. Note that these rates are clearly not proportional to the ion charge z.

Precautions in these decay measurements was taken to ensure that the sequential resonant ejection of different charge states with comparable mass results in quantitative ion detection. Within the trap, space charge fields couple the overlapping ion clouds of different species. As a result, the ejection of a dense inner cloud of low m/z ions through a surrounding cloud of higher m/z can destabilize the outer cloud and affect the quantitative detection of the higher m/z species. This is evident in Fig. 2 as larger scatter in the C_{60}^{+} signal at short exposure times when comparable quantities of C_{60}^{2+} are present. These effects were minimized by loading smaller initial quantities (< 1000) of the lower m/z ions. Decay rates were determined from ion data which did not exhibit large fluctuations, such as the $z=2$ and $z=3$ decays and data taken at longer exposure times for $z=1$ as shown in Fig. 2. As a final confirmation that the analysis yielded reliable rates, the decay rates of individually trapped ion species were compared with the rates obtained from a multiply-charged mass spectrum and found to be the same within experimental uncertainty.

3. Collision model

The Langevin model [6,7] is a useful starting point to describe thermal energy collisions between an ion and a polarizable neutral particle. Charge-exchange collision rates between C_{60}^{+} and alkali atoms at thermal energies have been shown [1] to scale with polarizability and reduced mass as predicted by the Langevin model [6,7]. However these measurements exhibited larger rates than this model estimates. In this model, the neutral is attracted by a charge–induced dipole interaction which results in a capture trajectory for impact parameters less than a critical value b^* determined by the collision energy E_0 and neutral polarizability α. However, the collision separation at which charge-exchange occurs r_c is determined by the specific potential curve crossing involved. It is useful to compare r_c with b^* to obtain a clearer interpretation of the collision process. For the collision models described below, the calculated critical impact parameters were in the range $b^* \approx 10$–20 Å. The neutral–ion separation at the curve crossing can be estimated as in Ref. [8] for collisions involving multiply-charged ions at thermal energies. For collisions of C_{60}^{2+} with Li, we estimate a crossing separation of $r_c \approx 5$–7 Å from ion center, assuming two point charges on the ion surface. Consequently, in the present experiments, b^* is sufficiently greater than r_c that the collision rates are expected to be more dependent on the ion charge distribution through the ion–neutral interaction than on details of the charge-exchange curve crossing. This is in contrast to the measurements determining details of C_{60}^{z+} fission energetics [4] and charge-exchange measurements of C_{60}^{2+} with C_{60} at high collision energies [9] both of which are more strongly dependent on the details of the charge dynamics at the point of charge-exchange. As a result of these considerations, the following analysis will concentrate on characterizing the dependence of the long range charge–induced dipole interaction on the ion charge distribution. Decay rate measurements will be compared with calculated collision rates derived from different assumptions of this charge distribution.

In the case of multiply-charged ions, the Langevin model predicts collision rates proportional to ion charge z. However, as indicated in Fig. 2, the measured relative decay rates of C_{60}^{3+}, C_{60}^{2+} and C_{60}^{+} are clearly inconsistent with this simple Langevin model. Considering that the diameter of C_{60}^{z+} (≈ 7 Å) is only a factor of 2–3 smaller than the critical impact parameter b^*, we propose that this departure from the Langevin model arises from an increased sensitivity to the nonuniformity of the ion charge distribution. As will be discussed more thoroughly below, a nonuniform ion charge distribution can arise from Jahn–Teller distortions of the icosahedral ion structure. Consequently, an analysis of the collision process will require a more detailed description of the ion charge distribution.

In many environments C_{60} behaves as a delocalized π-electron system with a polarizability comparable to that of a metal sphere of the same diameter [10]. If C_{60}^{z+} is modeled as a rigid metallic sphere of 3.55 Å radius, during the collision it becomes polarized by the fields of the induced dipole giving rise to an induced charge which is nonuniformly distributed on the microsurface. However, this nonuniformity was calculated and found to produce insignificant deviations from the Langevin cross sections ($< 1\%$) for impact parameters comparable to $b^* \approx 15$ Å.

In order to consider greater variations in the charge distribution, we chose to construct a distribution based on an assembly of point charges. Minimal energy configurations for a set of like charges on the surface of a sphere have been considered previously [11] and recently applied to charge-exchange [3], electrochemical reduction [12] and dissociation [4] of C_{60}^{z+}. Only the simpler geometries for 2 charges at opposite ends of a diameter, and 3 charges at the vertices of an equilateral triangle will be relevant to our analysis of doubly and triply ionized species. We present the following modifications of the Langevin model which involve point charge approximations of the charge distribution. Although each distribution is based upon a minimal energy configuration, these alternative models cover the two extremes of fixed and mobile charges.

3.1. Stationary charges

In contrast to the metallic model, we assume that the z charges are localized to points on the C_{60}^{z+} surface. The collision model based on this distribution was evaluated by explicitly integrating the trajectory to determine the cross section. To accomplish this, forces were computed for the charge–induced dipole configuration as shown in Fig. 3 for $z = 3$. Charges on C_{60}^{3+} with radius R induce a dipole p on the neutral particle of polarizability α. The induced dipole is expressed in terms of the net field from the point charges, $\boldsymbol{p} = \alpha \boldsymbol{E} = \alpha \sum \boldsymbol{E}_i$. The potential energy V is expressed by

$$V = -\frac{\boldsymbol{p}\cdot\boldsymbol{E}}{2} = -\frac{\alpha e^2}{2}\sum_i \left[\frac{1}{r_i^4} + \sum_{j\neq i}\frac{\boldsymbol{n}_i\cdot\boldsymbol{n}_j}{(r_i r_j)^2}\right], \tag{2}$$

and the force $\boldsymbol{F}_i$ on m due to the charge located at $\boldsymbol{r}_i$ is given by

$$\boldsymbol{F}_i = \boldsymbol{n}_i \alpha e^2 \sum_j \left[\frac{3\boldsymbol{n}_i\cdot\boldsymbol{n}_j}{r_i^3 r_j^2} - \frac{1}{r_i^2 r_j^3}\right], \tag{3}$$

where $\boldsymbol{n}_i$ is a unit vector in the direction of $\boldsymbol{r}_i$. The total force is then given by $\boldsymbol{F} = \sum_i \boldsymbol{F}_i$ and the resulting ion rotation follows from the torque equation,

$$\boldsymbol{T} = \sum_i \boldsymbol{R}_i \times \boldsymbol{F}_i .$$

To determine the cross sections for each charge state $z = 1$–3, a particular orientation of the charge distribution was selected and the critical impact parameter b^* was determined from the outcome of successive trajectories which varied the impact parameter. This evaluation was repeated for random selections of orientation and initial velocity in a Monte Carlo fashion to average the cross section

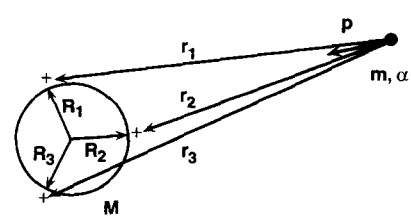

Fig. 3. The model geometry used to describe the interaction of C_{60}^{3+} having mass M with a neutral species of mass m and polarizability a is shown. Point charges are positioned on the ion microsurface at radii R_i and angular separations which minimize the repulsive Coulomb interaction. The interaction potential between the point charges and the induced dipole moment, p, is defined in Eq. (2).

over all orientations and the velocity distribution of the neutral beam. This average cross section $\langle \sigma_z \rangle$ is then related to the collision rate

$$k_z = \int_0^\infty \sigma_z(v)_v \, d\Phi_v = \langle \sigma_z \rangle \int_0^\infty d\Phi_v ,$$

where $d\Phi_v$ is the neutral flux for atoms with speeds between v and $v + dv$.

It is essential to point out here that rotational averaging of the ion charge distribution and the resulting charge–neutral interaction will not occur during the collision trajectory of alkali atoms or C_{60} since the rotational period of ≈ 20 ps at 300 K is a factor of ≈ 30 longer than the collision duration for Li, and a factor of ≈ 3 for C_{60}.

3.2. Mobile charges

In this case, the charges are considered sufficiently mobile for the distribution to maintain an orientation determined by the induced dipole. Such a model is based on the assumption that the net torque exerted by the induced dipole on the charges is capable of maintaining the distribution of point charges in the lowest energy configuration. In this configuration, one charge is oriented nearest the dipole throughout the neutral trajectory and the remaining charges are positioned to minimize the repulsive energy but otherwise free to rotate about the collision line of centers. In this orientation, the net force is a central force so that the net torque vanishes and calculation of the collision cross section reduces to the solution of a quartic equation which can be performed without the need for Monte Carlo methods. However, the calculations were performed both ways as a check on the Monte Carlo asymptote, and very close agreement was found.

4. Results and discussion

The relative rates k_z/k_1 for Li and Cs collisions with C_{60}^{z+} are compared in Fig. 4. Rates calculated with the stationary charge model are observed to agree closely with those calculated by the Langevin model. This was found to be the case even for the absolute rates with different z. This is a consequence of averaging over random orientations which yields an effective spherical charge distribution. In general,

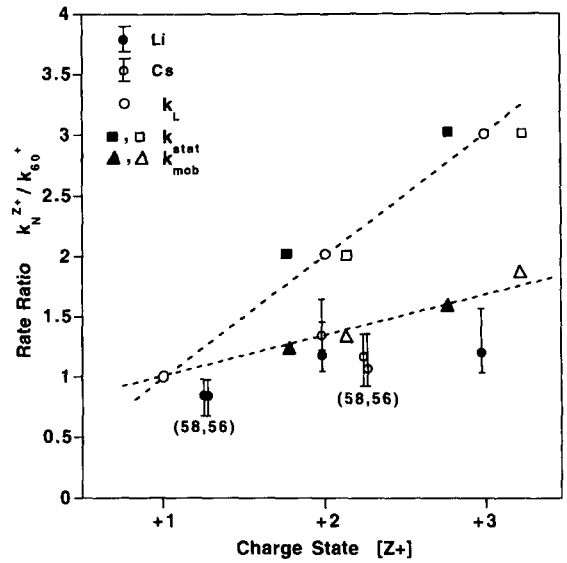

Fig. 4. A plot of experimental ratios of decay rates for multiply-charged ions is compared with calculations based on different models of the ion charge distribution. The data indicated by filled circles refer to Li measurements and open circles to Cs measurements of C_{60}^{z+} decay rates. Several decay measurements for fragments C_{56}^{z+} and C_{58}^{z+} are also shown. Calculated ratios indicated by open circles refer to the Langevin model, filled (open) squares to Li (Cs) decay in the stationary charge model and filled (open) triangles to Li (Cs) decay in the mobile charge model. Symbols refer to each individual charge state but are offset from the x-axis marker for clarity. Dashed lines are guides for the eye indicating trends of the model calculations.

any model relying on a stationary charge distribution will approach the Langevin result after such averaging over random orientations. However, the experimental measurements are in sharp disagreement with both these calculations.

Relative rates for the mobile charge model are also shown in Fig. 4 and these calculated rates display close agreement with experimental results. Collisions of Li and Cs with C_{58}^{z+}, C_{56}^{z+} fragments demonstrate similar agreement with the mobile model calculations. Charge-exchange collisions of C_{60}^{z+} with neutral C_{60} were also measured. It was observed that the charge-exchange of C_{58}^{2+} with C_{60} resulted in *equal* product densities of C_{60}^{+} and C_{58}^{+} confirming that stable products are formed in these collisions between heavy particles. In addition, the symmetric exchange of C_{60}^{+} with C_{60} was observed to occur without loss of C_{60}^{+} so that only the loss rates for C_{60}^{3+} and C_{60}^{2+} could be determined. The ratio of

these rates was measured to be $(k_3/k_2) = 1.38 \pm 0.08$ and the mobile charge model yields a ratio of 1.37, in close agreement with measurement. It is evident that motion of the charge distribution during the trajectory plays an essential role in the physics of this collision process and that a nonuniform charge distribution alone is not sufficient to explain this phenomena.

As shown in Fig. 4, both measurements and mobile model calculations exhibit relative rates only fractionally larger than unity, which suggests that the single charge nearest the neutral during the trajectory effectively determines the collision rate. The absolute rates calculated for Li collisions with the mobile charge model are larger than the Langevin rates by a factor of 2.1 for C_{60}^{+}, 1.3 for C_{60}^{2+} and 1.1 for C_{60}^{3+}, and similar results were found for Cs. This result is expected as the multiply-charged ions more closely approximate a uniform charge distribution with increasing z. These calculations are consistent with previous measurements [1] of alkali charge-exchange with C_{60}^{+} which indicated absolute rates in excess of the Langevin model by a factor of 2–3. Bohme [2,13] also measured occasional ion–neutral collision rates larger than Langevin rates for collisions of C_{60}^{+} and C_{60}^{2+} with several organic species.

Delocalized charges on the C_{60}^{z+} ion surface have been neglected in our calculations. Dielectric screening by these charges would reduce the fields at the position of the neutral leading to a smaller induced dipole and as a result slower collision rates. In the stationary charge model, the average over random orientations will tend to average out screening effects in the relative rates. However, in the mobile charge model for $z = 1$–3, only the closest charge contributes significantly to the induced dipole, so that the effect of screening will be roughly independent of z. In this case, the relative rate analysis depending on rate ratios would be insensitive to the presence of screening. Furthermore, C_{60}^{z+} fission measurements [4] indicate that screening effects were observed only for $z \geqslant 6$.

It is also important to point out that the charge-exchange collisions studied here with $z > 1$ occur without an energy barrier imposed by Coulomb repulsion [2,3]. The estimated ion–neutral separation at the charge-exchange curve crossing of $r_c \approx 5$–7 Å and the neutral ionization potentials of Cs (3.9 eV), Li (5.4 eV) and C_{60} (7.6 eV) result in an exothermic process which probably leaves the $C_{60}^{(z-1)+}$ ion in an excited electronic state.

The close agreement observed between the theoretical model and measured collision rates is surprising since the ability for charge to freely move about on the ion surface would seem to be inconsistent with the presence of a nonuniform charge distribution. However, such a model of the charge dynamics becomes quite plausible upon considering the consequences of both static and dynamic Jahn–Teller effects in C_{60}^{z+}. Recent ab initio calculations have shown that both positive [14] and negative [15] ions of C_{60} with open electronic shells undergo static Jahn–Teller distortions which lower the icosahedral symmetry of the neutral molecule. These distortions are predicted to introduce changes in the bond lengths and associated charge distributions near an equator of the molecular cage. The ion models introduced here which treat point charges confined to the spherical surface may be considered as a simple representation of these distortions. Dynamic Jahn–Teller effects have been indicated in photoemission measurements [16] of C_{60}^{-} and also as the basis for the weak temperature dependence of electron paramagnetic resonance (EPR) spectra of triplet state C_{60} [17–19]. The EPR linewidth variation with temperature is characteristic of a rotation of the symmetry axis about the direction of the magnetic field. This observation is interpreted to result from rapid ($\approx 10^{-14}$–10^{-13} s) tunneling [19] among nearly degenerate vibronic states associated with different symmetry axes. In the case of C_{60}^{z+} collisions, a similar tunneling among states with different axes of molecular symmetry could reorient the charge inhomogeneity during the collision trajectory. Such a pseudorotation of the charge distribution would provide the apparent charge mobility suggested by our collision model. Further investigations are planned to detect the presence of dynamic Jahn–Teller effects in collisions by measuring the dependence of the collision rates on the vibrational temperature of trapped C_{60}^{z+} over a range of 10 to 300 K.

To summarize, charge-exchange collisions of C_{60}^{z+} with both alkali atoms and C_{60} are observed to occur with rates which are relatively insensitive to the charge state. This result contradicts calculations based upon a uniform charge distribution including the

standard Langevin model. A theoretical model which closely predicts measurements of the relative rates incorporates an array of point charges on the C_{60}^{z+} surface to approximate the nonuniform distribution. In addition, the model includes the property of charge mobility which allows the distribution to reorient during the collision trajectory. These characteristics of charge localization and mobility, although seemingly contradictory, are both required in the collision model to describe experimental results. Jahn–Teller effects including distortion of the ion charge distribution as well as a pseudorotation of this distribution yield a plausible basis for the physics characterized by the model.

Acknowledgements

We would like to thank Michael Burns, Mordechai Rokni and Abraham Szöke for relevant discussions during the progress of this work. This research was fully supported by The Rowland Institute for Science.

References

[1] S. Pollack, D. Cameron, M. Rokni, W. Hill, J.H. Parks, Chem. Phys. Lett. 256 (1993) 473.
[2] S. Petrie, G. Javahery, J. Wang, D.K. Bohme, J. Phys. Chem. 96 (1992) 6121.
[3] S. Petrie, J. Wang, D.K. Bohme, Chem. Phys. Lett. 204 (1993) 473.
[4] P. Scheier, B. Dünser, T.D. Märk, J. Phys. Chem. 99 (1995) 15428.
[5] J.H. Parks, S. Pollack, W. Hill, J. Chem. Phys. 101 (1994) 6666.
[6] P. Langevin, Ann. Chim. Phys. 5 (1905) 245, and an English translation which appears in: E.W. McDaniel, Collision Phenomena in Ionized Gases, Wiley, New York, 1964, p. 701.
[7] G. Gioumousis, D.P. Stevenson, J. Chem. Phys. 29 (1958) 294.
[8] A. Salop, R.E. Olson, Phys. Rev. A 13 (1976) 1312.
[9] F. Rohmund, E.E.B. Campbell, Chem. Phys. Lett. 245 (1995) 237.
[10] G.F. Bertsch, A. Bulgac, D. Tomanek, Y. Wang, Phys. Rev. Lett. 67 (1991) 2690.
[11] H.A. Munera, Nature 320 (1986) 597.
[12] R.S. Ruoff, P.L. Boulas, K.M. Kadish, Y. Wang, Electrochem. Soc. Proc. 95-10 (1995) 287.
[13] G. Javahery, H. Wincel, S. Petrie, D.K. Bohme, Chem. Phys. Lett. 204 (1993) 467.
[14] J. Cioslowski, S. Patchkovskii, W. Thiel, Chem. Phys. Lett. 248 (1996) 116.
[15] V. de Coulon, J.L. Martins, F. Reuse, Phys. Rev. B 45 (1992) 13671.
[16] O. Gunnarsson, H. Handschuh, P.S. Bechthold, B. Kessler, G. Ganteför, W. Eberhardt, Phys. Rev. Lett. 74 (1995) 1875.
[17] M. Bennati, A. Grupp, M. Mehring, J. Chem. Phys. 102 (1995) 9457.
[18] X. Wei, Z.V. Vardeny, Phys. Rev. B 52 (1995) R2317.
[19] G.L. Closs, P. Gautam, D. Zhang, P.J. Krusic, S.A. Hill, E. Wasserman, J. Phys. Chem. 96 (1992) 5228.